

P.J. Bryant and R. Perin
CERN
Geneva, Switzerland

Summary

The Split Field Magnet (SFM) is a general purpose spectrometer which has been functioning in an intersection of the CERN Intersecting Storage Rings (ISR) since summer 1973. Its equivalent field volume of $28 \text{ T}\cdot\text{m}^3$ is crossed by the two circulating ISR proton beams. The bending action is compensated by two additional magnets per beam, and the focusing ($\sim 2.4 \text{ T}$ of integrated field gradient) by adjustable passive beam channels. The residual magnetic field effects were studied for tune changes across the aperture and the excitation of non-linear resonances, especially as the machine superperiodicity is reduced to one. Details are presented of these effects and of their compensation. The luminosity in the SFM is reduced by $\sim 18 \%$ due to an increase in the crossing angle of the beams, but the influence of the other factors has been limited to a few percent. Except for tune changes of the order of 0.004, which require minor modifications of working lines at the lower energies, and a small influence on high precision closed orbit bumps used for luminosity measurements, the ISR behave as if the SFM were not present. No operational restrictions have been encountered and all special facilities, such as acceleration to $31 \text{ GeV}/c$ by phase displacement, remain unaffected.

1. Introduction and General Description

The Split Field Magnet, so called because it produces fields of opposite sign on either side of its vertical symmetry plane, is a large magnetic spectrometer installed in an intersection region of the ISR. The main requirements of the experimentalists were a large volume of magnetic field covering the full solid angle around the intersection and a bending power of at least $4 \text{ T}\cdot\text{m}$ in the forward beam directions. This field acts directly on the ISR beams.

With respect to the ISR machine, the system had to disturb the circulating beams as little as possible and had to be such that it could be switched off without hampering the regular operation. This implied that the existing ISR magnet structure could not be altered.

The above mentioned requirements led to a design which includes a number of unconventional solutions such as the pentagonal shape of the main magnet, the absence of a yoke to carry the return flux and to withstand the magnetic forces, the magnetic channels to protect the proton beams over part of their way through the magnet and the need to assemble completely the magnet outside the ISR and to transport it as a single unit to its working place.

A general layout of the installation is shown in Figure 1. Each proton beam passes through an upstream compensator, the main magnet and a downstream compensator magnet. The main magnet can be regarded as composed of two horseshoe type magnets equidistant from the horizontal symmetry plane. At the beam crossing point, the magnetic field is zero and has opposite signs upstream and downstream of that point. The force of attraction between the poles and the weight of the top yoke and coils are supported by four pillars made from non-magnetic steel. Magnetic channels screen the

ISR beams from the defocusing effects of the upstream edges of the magnet and compensate those occurring in its central part. They have the form of long rectangular tubes and are made from low carbon steel and aluminium. Their cross-section varies from point to point along their length in order to cope with the different field intensities and gradients. Over the last half meter, near to the beam intersection, the channels are provided with horizontal plates called "trim flaps" that can be inclined at a variable angle to the horizontal. With the trim flaps it is possible to produce, at will, field gradients to adjust the behaviour of the channels for different field levels and to compensate the edge focusing at the intersection.

The large compensators are H-type magnets with asymmetric return yokes. Besides compensating the deflection of the ISR beams, they are used for the analysis of high momentum particles produced at small angles. The small compensators are short window-frame magnets. All magnets are aligned in the ISR with an accuracy of 0.1 mm .

Table 1 summarizes the main features of the magnets.

TABLE 1

<u>Main Magnet (SFM)</u>			
- Nominal induction in median plane			1.14 T
- Gap height			1.10 m
- Length			10.50 m
- Width	at the end		2.00 m
	at the centre		3.50 m
- Weight			900 t
- Nominal power			4 MW
<u>Compensators</u>		<u>Large</u>	<u>Small</u>
- Nominal induction in median plane	(T)	1.5	1.8
- Gap height	(m)	0.4	0.075
- Steel length	(m)	1.5	0.435

2. Criteria Used in the Design and Assessment of the SFM

Every effort was made in the SFM design to minimize the loss of luminosity and the degradation of the ISR beams. For bending effects, this entails careful adjustment of the compensator magnets to prevent the residual orbit distortion from decreasing the maximum stack width. The local loss of luminosity of 18% in the SFM itself, which arises from an increase in the beam crossing angle, is unavoidable. To evaluate the impact of the focusing effects on the whole ISR, the fractional

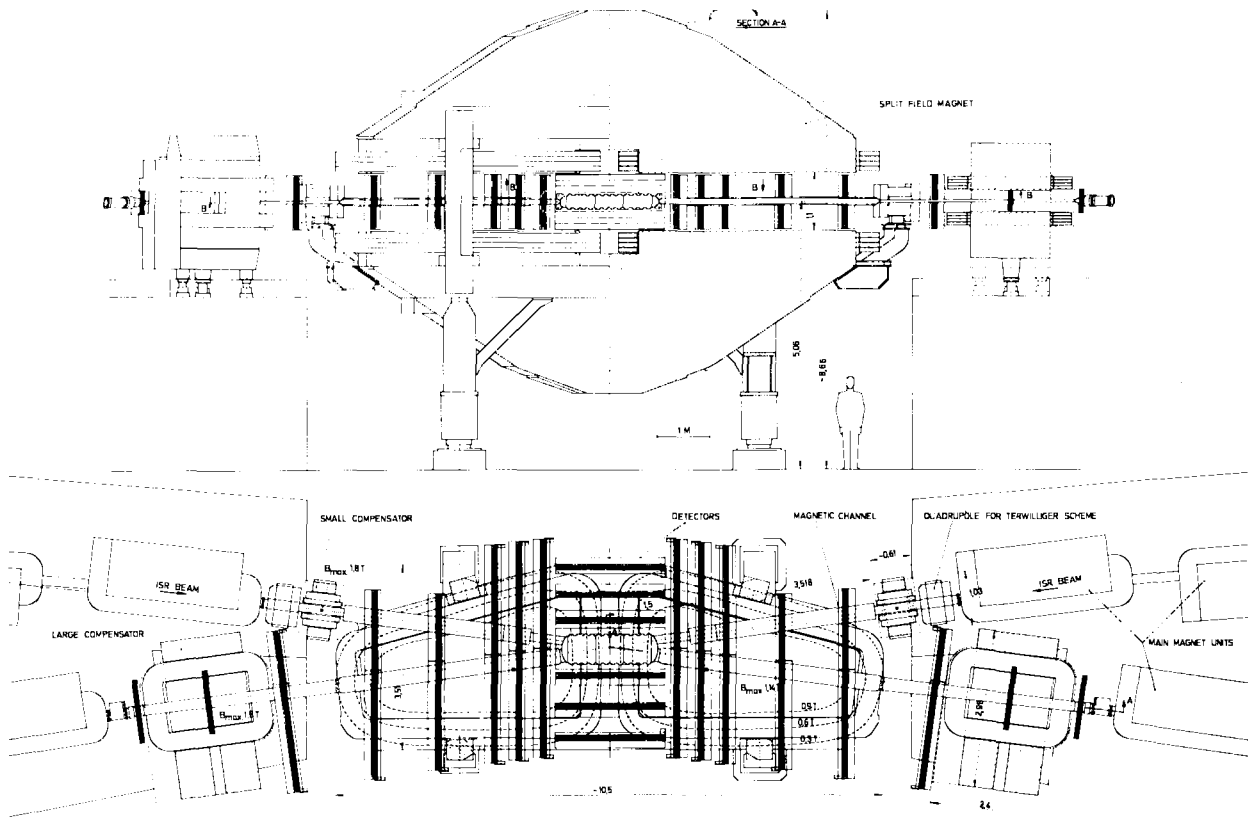


Figure 1. Schematic Layout of the Split Field Magnet Facility in the Intersection Region I4

change in a notional maximum luminosity was used, which assumes the vacuum chamber to be entirely filled by the beam². This reduction of luminosity arises from an increased modulation of the momentum compaction function and from increased horizontal and vertical betatron oscillation amplitudes.

Finally, the effects of non-linear resonances have been estimated and evaluated in terms of the existing excitations in the ISR.

3. Bending Effects

Figure 2 shows the closed orbits in the SFM system with reference to the undisturbed beam trajectories. The compensator settings were calculated from the magnetic measurements at each field level. A mismatch of only 38 Gm at 25 GeV/c is sufficient to create a residual distortion in the ISR of ± 1 mm peak-to-peak. As can be seen from Table 2, this limit has been respected and, in most cases, improved upon. This level of distortion can be safely tolerated.

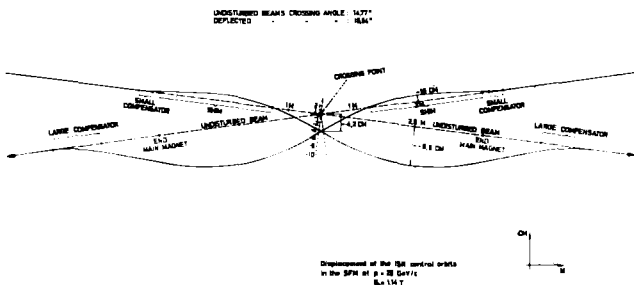


Figure 2. Displacement of the ISR central orbits in the SFM at $p = 25$ GeV/c and $B_0 = 1.14$ T.

TABLE 2

Residual Closed Orbit Distortion Added to ISR

Energy GeV/c	26.588	22.505	15.376	11.780
Horizontal orbit distortion peak-to-peak	± 0.5 mm	± 0.65 mm	---	± 1.1 mm

4. Focusing Effects

The beam enters the SFM on the upstream side at an angle of $\sim 20^\circ$ to the pole edge and crosses the central region at $\sim 80^\circ$ to the plane of the field reversal (see Figure 1). At full field, the integrated transverse gradients in these regions are 2 T and 0.3 T, respectively (see Figure 3). According to the criterion mentioned in section 2, these gradients, if uncompensated, would cause 87 % loss in luminosity. The use of a compensating quadrupole directly upstream of the small compensator could reduce this loss to 35 %. This was still felt to be too high, especially since the luminosity in the SFM itself is further reduced by 18 % due to the increased crossing angle. For this reason, magnetic channels were adopted although they obstruct somewhat the physics equipment and create showers of secondary particles. Despite the widely different degrees of saturation in the magnetic channels between the maximum and minimum field levels, the transverse gradient seen by the beam when crossing the pole edge is virtually eliminated. The central gradient is compensated by the trim flaps. The overall effects at full and half field are shown in Figure 4.

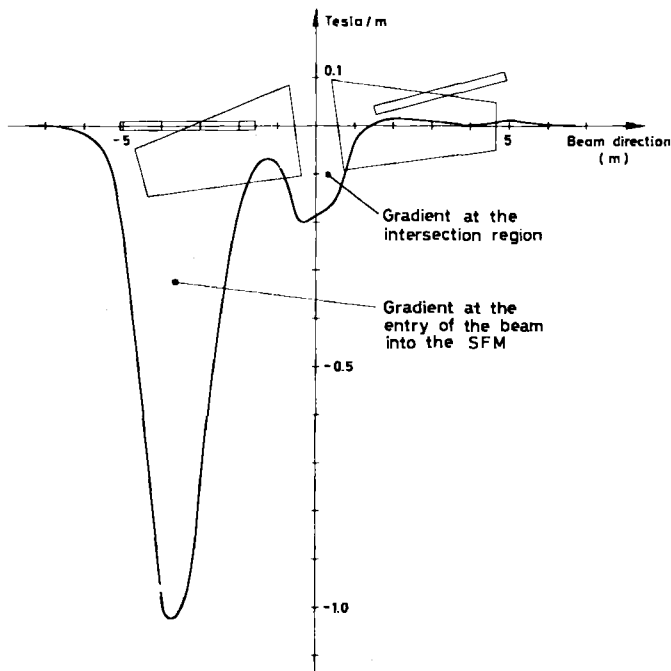


Figure 3. Transverse gradient without magnetic beam channels at maximum field level.

The small field gradients acting on the beam in the downstream half of the SFM depend upon the radial position of the magnet. Using the measurements made at full and half field on a fifth scale model, the variation of luminosity with the radial position of the SFM was evaluated in order to find the best balance between the various regions of gradient. On the basis of these calculations, it was decided to place the SFM so that its geometrical centre was shifted by 10 cm to the inside of the ISR with respect to the undisturbed beams' crossing point. Under these conditions, the loss in luminosity was estimated at 7 - 9 %.

A tracking program, using the magnetic measurements made at each field level, was used to integrate the residual field components along the beam trajectory. Table 3 summarizes the results for the central orbit and Table 4 gives the changes in the beam parameters derived from these measurements.

TABLE 3

Integrals of quadrupole and sextupole components along the beam trajectory (Ring 1)

SFM field level (T)	Corresponding momentum (GeV/c)	Integrated quadrupole (T)	Integrated sextupole (T/m)
1.14	26.588	- 0.0117	- 1.103
1.00	22.505	- 0.0056	- 1.141
0.65	15.376	0.0	- 0.900
0.50	11.780	- 0.0028	- 0.767

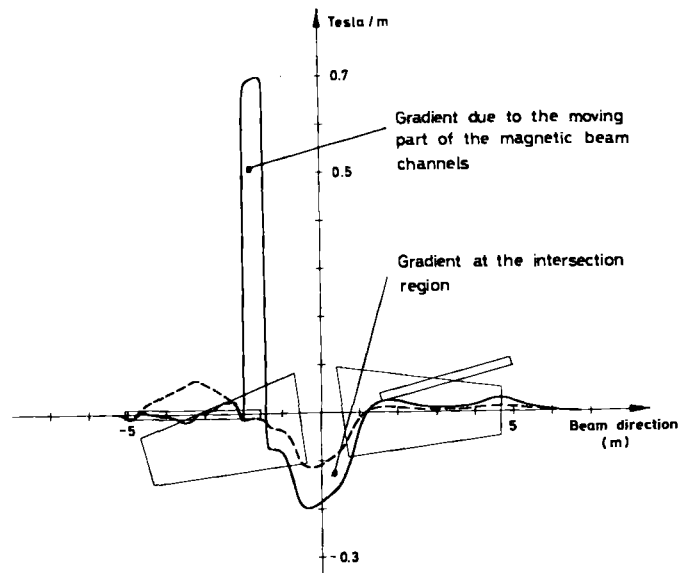


Figure 4. Transverse gradient with magnetic beam channels at :
 - maximum field level (—————)
 - half field level (-----)

TABLE 4

Computed changes of ISR parameters with the SFM

	SFM field level (T)			
	1.14	1.00	0.65	0.50
	Corresponding momentum (GeV/c)			
	26.588	22.505	15.376	11.780
ΔQ_H	0.0003	0.0003	0.0001	0.0001
ΔQ_V	0.0014	0.0015	0.0014	0.0012
$\Delta Q_H'$	0.048	0.060	0.076	0.082
$\Delta Q_V'$	- 0.030	- 0.038	- 0.044	- 0.048
$\Delta \beta_{H,max}$	0.07	0.06	0.08	0.12
$\Delta \beta_{V,max}$	0.67	0.80	0.85	0.86
$\Delta \alpha_{p,max}$	0.006	0.008	0.006	0.005
$\frac{L(S)}{L(O)}$	0.966	0.960	0.960	0.966

where :

- $\Delta Q_H, \Delta Q_V$ are the changes in horizontal and vertical tunes,
- $\Delta Q_H', \Delta Q_V'$ are the changes in horizontal and vertical tune spreads,
- $\Delta \beta_{H,max}, \Delta \beta_{V,max}$ are the changes in the maximum horizontal and vertical betatron amplitude functions,
- $\Delta \alpha_{p,max}$ is the change in the maximum momentum compact-ion function.
- $\frac{L(S)}{L(O)}$ is the fractional change in the luminosity due to the changes in β_H, β_V and α_p . "S" signifies the presence of the SFM and "O" its absence.

The parameter changes and loss of luminosity calculated in Table 4 are so small as to be practically unmeasurable in the machine and indeed the ISR performance has shown no degradation. However, it has been found necessary to make some minor tune changes (0.004) at injection to the ISR working lines at 11, 15 and 22 GeV/c and to modify by 1 - 2 % the excitation of the dipole magnets for the high-precision, vertical bumps used in the SFM itself for luminosity measurements.

5. Higher Order Effects

Equation (1) is the general condition for a non-linear resonance

$$n_1 Q_H + n_2 Q_V = p \quad (1)$$

where :

$(n_1 + n_2) = N$, the order of the resonance,

p is the order of azimuthal harmonic of the magnetic imperfection exciting the resonance.

In the case of the SFM, the field on the median plane is purely vertical. This limits the resonances, which can be excited, to those for which n_2 is even. The measurements cannot give reliable results beyond the octupole term, so it is not possible to calculate the resonance excitation for the SFM beyond the 4th order resonances. A coefficient of excitation, d_p , can be defined for a series of, m , localized errors:

$$|d_p| = \frac{1}{C} \left| \sum_m \beta_{H,m}^{n_1/2} \beta_{V,m}^{n_2/2} e^{i(n_1 \mu_{H,m} + n_2 \mu_{V,m})} \left(\frac{\partial^{N-1} B_z}{\partial x^{N-1}} \right)_m \right| \quad (2)$$

(for n_2 even)

where :

$\mu_{H,m}, \mu_{V,m}$ are the betatron phases in the m^{th} region

l_m is the length of the m^{th} field error

C is the machine circumference

B_z is the vertical field

The SFM was sub-divided along the trajectory and the excitation coefficients as given by equation (2) were evaluated for the 3rd and 4th order resonances. The results are summarized in Table 5. These calculations are based on the intermediate field level of 0.65 T with a beam momentum of 15 GeV/c.

To give some idea of the meaning of these coefficients, the coefficient for the 4th order resonances ($N = 4, n_1 = 4, n_2 = 0$) arising from the main ISR magnet is ~ 3 . Thus, the SFM adds approximately the same order of magnitude to the resonance excitation as the ISR main magnet. However, the beam-beam excitation of resonances is an order of magnitude stronger and remains the dominant effect. The limitation to 4th order resonances, imposed by the accuracy of the magnetic measurements, left some uncertainty as to the higher order resonance excitations. Subsequent operation with the ISR has given no evidence of extra excitation arising from the SFM.

TABLE 5

The SFM excitation coefficients for 3rd and 4th order resonances on the equilibrium orbits for momentum deviations, $\Delta p/p = -3\%, 0, +3\%$

(SFM field level = 0.65 T and beam momentum = 15 GeV/c)

Orbit $\Delta p/p$	Order of resonances			Excitation $ d_p $
	n_1	n_2	N	
0.0	1	2	3	0.0
	3	0	3	0.0
	2	2	4	0.8
	4	0	4	1.1
	0	4	4	0.6
+ 3 %	1	2	3	0.0
	3	0	3	0.0
	2	2	4	1.4
	4	0	4	1.7
	0	4	4	1.2
- 3 %	1	2	3	0.0
	3	0	3	0.0
	2	2	4	6.1
	4	0	4	6.9
	0	4	4	5.5

6. ISR Performance with the SFM

No operational restrictions have been imposed on the ISR due to the SFM. The special facilities of acceleration to 31 GeV/c by phase displacement and the superposition of the equilibrium orbits to create small interaction diamonds are both fully compatible. The loss in the notional, maximum luminosity is a somewhat artificial parameter which served as a design criterion. In practice the loss of luminosity is so small as not to be apparent except for the already mentioned 18 % reduction in the SFM itself. Physics conditions are also equally as good with the SFM as without it. The insensitivity of the ISR to the SFM's presence has been a very great advantage in the scheduling of physics experiments. The most recent run used 10.6 A beams, which had a starting luminosity of $3.2 \times 10^{30} \text{ cm}^{-2} \text{ sec}^{-1}$ in the SFM and an average decay rate of 10^{-6} min^{-1} over the 27 hours of the run.

Acknowledgements

The authors would like to thank all the people in the CERN ISR division who have contributed to the SFM project.

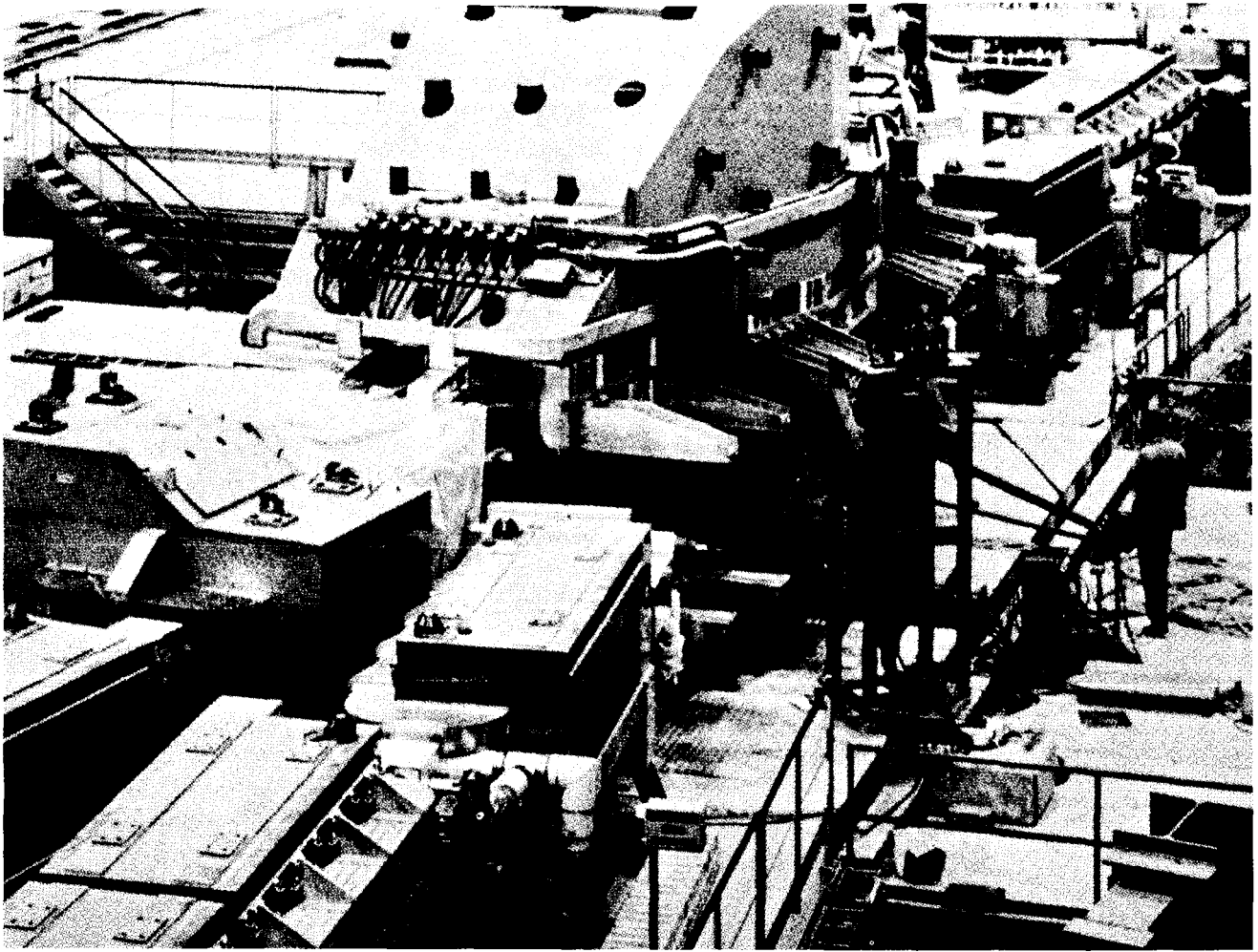


Figure 5. The SFM spectrometer installed in the ISR

References

- 1) J. Billan, R. Perin, V. Sergo - The Split Field Magnet of the CERN Intersecting Storage Rings - Proc. 4th Int. Conf. on Magnet Technology, Brookhaven (1972).
- 2) B. Couchman, B. de Raad, P. Strolin - Calculation of orbit perturbations and some remarks concerning the magnet system proposed for ISR experiments - ISR Divisional Report ISR-BT/68-57 (1968).
- 3) G. Guignard - Effets des Champs Magnétiques Perturbateurs d'un Synchrotron sur l'Orbite Fermée et les Oscillations Bétatroniques, ainsi que leur Compensation - Report CERN 70-24 (1970).
- 4) E. Keil - A comparison of non-linear resonances excited by magnet imperfections and by beam-beam space charge forces - (or Why be afraid of magnet imperfection resonances in high luminosity storage rings ?) - ISR Divisional Report ISR-TH/73-25 (1973).